

Supplement: Meltwater generation in ice stream shear margins: case study in Antarctic ice streams

Meghana Ranganathan¹, Jack William-Barotta^{2,3}, Colin R. Meyer⁴, Brent Minchew¹

¹*Department of Earth, Atmospheric and Planetary Sciences, Massachusetts Institute of Technology, Cambridge, MA, USA*

²*Department of Mathematics, Massachusetts Institute of Technology, Cambridge, MA, USA*

³*School of Engineering, Brown University, Providence, RI, USA*

⁴*Thayer School of Engineering, Dartmouth College, Hanover, NH, USA*

Correspondence: Meghana Ranganathan <meghanar@mit.edu>

CONTENTS

Section A: Derivations	2
Nondimensionalization	2
Higher-Order Matching to Find Inner Solution of Porosity, ϕ_1	4
Finding Composite Solutions	6
Section B: Comparison to Numerics for Different Shear Heating Rate	7
Section C: Dependence of Temperature, Pressure, Porosity, and Flux on Various Parameters	9
Section C: Effect of κ on depth profiles	11
Section D: Effect of Temperature-Varying A	11
Section E: Brinkman and Peclet Numbers in Ice Streams	12

21 **SECTION A: DERIVATIONS**22 **Nondimensionalization**

23 Let

$$\begin{aligned}
\tilde{\mathcal{H}} &= [\mathcal{H}]\mathcal{H} & [\mathcal{H}] &= \rho_I c_p \Delta T \\
\tilde{z} &= Hz \\
\tilde{T} &= [T]T + T_m & [T] &= \Delta T \\
\tilde{\phi} &= [\phi]\phi & [\phi] &= \epsilon = \frac{\rho_I c_p \Delta T}{\rho_w \mathcal{L}} \\
\tilde{N} &= [N]N & [N] &= \frac{[\eta_I] K \Delta T}{\epsilon \rho_w \mathcal{L} H^2} \\
\tilde{t} &= [t]t & [t] &= \frac{H^2 \rho_I c_p}{K}
\end{aligned}$$

24 We non-dimensionalize Equation (??):

$$\frac{[\mathcal{H}]}{[t]} \frac{\partial \mathcal{H}}{\partial t} + a \frac{[\mathcal{H}]}{H} \frac{\partial \mathcal{H}}{\partial z} - K \frac{[T]}{H^2} \frac{\partial^2 T}{\partial z^2} = W - \frac{\rho_w \mathcal{L} [\phi] [N]}{[\eta_I]} \phi N \quad (1)$$

$$\implies \frac{\partial \mathcal{H}}{\partial t} + a \frac{[t]}{H} \frac{\partial \mathcal{H}}{\partial z} - K \frac{[T][t]}{[\mathcal{H}]H^2} \frac{\partial^2 T}{\partial z^2} = W \frac{[t]}{[\mathcal{H}]} - \frac{\rho_w \mathcal{L} [t] [\phi] [N]}{[\eta_I] [\mathcal{H}]} \phi N \quad (2)$$

$$\implies \frac{\partial \mathcal{H}}{\partial t} + \left(\frac{a H^2 \rho_I c_p}{HK} \right) \frac{\partial \mathcal{H}}{\partial z} - \left(\frac{K \Delta T H^2 \rho_I c_p}{H^2 K \rho_I c_p \Delta T} \right) \frac{\partial^2 T}{\partial z^2} = \left(\frac{H^2 \rho_I c_p}{K \rho_I c_p \Delta T} \right) W - \left(\frac{\rho_w \mathcal{L} H^2 \epsilon \eta_I K \Delta T}{\eta_I K \Delta T \epsilon \rho_w \mathcal{L} H^2} \right) \phi N \quad (3)$$

$$\implies \frac{\partial \mathcal{H}}{\partial t} + \left(\frac{a H \rho_I c_p}{K} \right) \frac{\partial \mathcal{H}}{\partial z} - \frac{\partial^2 T}{\partial z^2} = \left(\frac{H^2}{K \Delta T} \right) W - \phi N \quad (4)$$

$$(5)$$

25 We define two nondimensional numbers:

$$\text{Br} = \frac{WH^2}{K\Delta T} \quad (6)$$

$$\text{Pe} = \frac{aH\rho_I c_p}{K} \quad (7)$$

26 So we can rewrite Equation (5) in terms of these numbers:

$$\frac{\partial \mathcal{H}}{\partial t} + \text{Pe} \frac{\partial \mathcal{H}}{\partial z} - \frac{\partial^2 T}{\partial z^2} = \text{Br} - \phi N \quad (8)$$

27 Now we non-dimensionalize Equation (??):

$$\frac{1}{H} \frac{\partial}{\partial z} \left\{ \frac{k_0([\phi]\phi)^\alpha}{\eta_w} \left[-(\rho_w - \rho_I)g + \frac{[N]}{H} \frac{\partial N}{\partial z} \right] \right\} = \frac{[\phi][N]}{\eta_I} \phi N \quad (9)$$

$$\implies \frac{k_0 \epsilon^\alpha}{H \eta_w} \frac{\partial}{\partial z} \left\{ \phi^\alpha \left[-(\rho_w - \rho_I)g + \frac{[N]}{H} \frac{\partial N}{\partial z} \right] \right\} = \frac{\epsilon [N]}{\eta_I} \phi N \quad (10)$$

$$\implies \frac{k_0 \epsilon^\alpha (\rho_w - \rho_I)g}{H \eta_w} \frac{\partial}{\partial z} \left\{ \phi^\alpha \left[-1 + \frac{[N]}{H(\rho_w - \rho_I)g} \frac{\partial N}{\partial z} \right] \right\} = \frac{\epsilon [N]}{\eta_I} \phi N \quad (11)$$

28 We multiply both sides by $\frac{\rho_w \mathcal{L} H^2}{\Delta T K}$:

$$\left(\frac{\rho_w \mathcal{L} H^2}{\Delta T K} \right) \frac{k_0 \epsilon^\alpha (\rho_w - \rho_I)g}{H \eta_w} \frac{\partial}{\partial z} \left\{ \phi^\alpha \left[-1 + \frac{[N]}{H(\rho_w - \rho_I)g} \frac{\partial N}{\partial z} \right] \right\} = \left(\frac{\rho_w \mathcal{L} H^2}{\Delta T K} \right) \frac{\epsilon [N]}{\eta_I} \phi N \quad (12)$$

$$\implies \frac{k_0 \epsilon^\alpha \rho_w \mathcal{L} H (\rho_w - \rho_I)g}{\eta_w K \Delta T} \frac{\partial}{\partial z} \left\{ \phi^\alpha \left[-1 + \frac{[N]}{H(\rho_w - \rho_I)g} \frac{\partial N}{\partial z} \right] \right\} = \frac{\rho_w \mathcal{L} H^2 \epsilon \eta_I K \Delta T}{K \Delta T \eta_I \epsilon \rho_w \mathcal{L} H^2} \phi N \quad (13)$$

$$(14)$$

29 Define two more non-dimensional numbers:

$$\delta = \frac{[N]}{H(\rho_w - \rho_I)g} \quad (15)$$

$$\kappa = \frac{k_0 \rho_I c_p \epsilon^\alpha (\rho_w - \rho_I)g}{\epsilon K \eta_w} \quad (16)$$

30 So we can rewrite Equation (14) in terms of these numbers:

$$\frac{\partial}{\partial z} \left\{ \kappa \phi^\alpha \left[-1 + \delta \frac{\partial N}{\partial z} \right] \right\} = \phi N \quad (17)$$

31 The non-dimensionalized equations are

$$\frac{\partial \mathcal{H}}{\partial t} + \text{Pe} \frac{\partial \mathcal{H}}{\partial z} - \frac{\partial^2 T}{\partial z^2} = \text{Br} - \phi N \quad (18)$$

$$\frac{\partial}{\partial z} \left\{ \kappa \phi^\alpha \left[-1 + \delta \frac{\partial N}{\partial z} \right] \right\} = \phi N \quad (19)$$

32 **Higher-Order Matching to Find Inner Solution of Porosity, ϕ_1**

33 Equation (??) can be used to find the first order solution for porosity from Equation (??). We can integrate

34 Equation (??) to obtain

$$\phi_1(\hat{z}) = \int \frac{\text{Br} - \phi_0 N_{\text{inner}}}{\text{Pe}} d\hat{z} \quad (20)$$

$$= \int \frac{\text{Br}}{\text{Pe}} - \frac{\phi_0}{\text{Pe}} [N_{\text{outer}}(0) + [N_0 - N_{\text{outer}}(0)] \exp[-\sqrt{a}\hat{z}]] d\hat{z} \quad (21)$$

$$= \int \frac{\text{Br} - \phi_0 N_{\text{outer}}(0)}{\text{Pe}} - \frac{\phi_0}{\text{Pe}} [N_0 - N_{\text{outer}}(0)] \exp[-\sqrt{a}\hat{z}] d\hat{z} \quad (22)$$

$$= \left[\frac{\text{Br} - \phi_0 N_{\text{outer}}(0)}{\text{Pe}} \right] \hat{z} + \frac{\phi_0}{\sqrt{a}\text{Pe}} [N_0 - N_{\text{outer}}(0)] \exp[-\sqrt{a}\hat{z}] + C \quad (23)$$

$$(24)$$

35 To find C , we use the higher-order matching condition

$$\lim_{\hat{z} \rightarrow \infty} \delta^\beta \phi_1(\hat{z}) = \lim_{z \rightarrow 0} \phi_{\text{outer}}(z) \quad (25)$$

36 First let's expand the outer solution for $z \rightarrow 0$. Consider Equation (??), the outer porosity equation. Let

37 $y = \phi_{\text{outer}}$ and expand y such that

$$y = y_0 + \frac{z}{z_{ct}} y_1 \quad (26)$$

38 We can expand Equation (??) as

$$\text{Pe}(y_0 + \frac{z}{z_{ct}} y_1) - \kappa(y_0 + \frac{z}{z_{ct}} y_1)^\alpha = \text{Br}(z - z_{ct}) \quad (27)$$

39 At zeroth order, we have $\text{Pe}y_0 - \kappa y_0^\alpha = \text{Br}(z - z_{ct})$, in which $y_0 = \phi_{\text{outer}}(0)$. At first order ($\mathcal{O}(\frac{z}{z_{ct}})$), we
40 have

$$\text{Pe}y_1 - \kappa\alpha y_0^{\alpha-1} y_1 = \text{Br}z_{ct} \quad (28)$$

$$\implies y_1 = -\frac{\text{Br}z_{ct}}{\kappa\alpha y_0^{\alpha-1} - \text{Pe}} \quad (29)$$

41 So we have

$$\lim_{z \rightarrow 0} \phi_{\text{outer}}(z) = \phi_{\text{outer}}(0) + \frac{z}{z_{ct}} \left[-\frac{\text{Br}z_{ct}}{\kappa\alpha y_0^{\alpha-1} - \text{Pe}} \right] \quad (30)$$

42 Now let's expand $\phi_1(\hat{z})$ for large \hat{z} . We note that $\hat{z} = \frac{z}{\delta^\beta}$ and we do a change of variables:

$$\lim_{z \rightarrow \infty} \int \delta^\beta \frac{\partial \phi_1}{\partial \hat{z}} d\hat{z} = \delta^\beta \left[\frac{\text{Br} - \phi_0 N_{\text{outer}}(0)}{\delta^\beta \text{Pe}} \right] \hat{z} + \lim_{z \rightarrow \infty} \delta^\beta \frac{\phi_0}{\sqrt{a} \text{Pe}} [N_0 - N_{\text{outer}}(0)] \exp\left[-\frac{\sqrt{a}}{\delta^\beta} z\right] + C \quad (31)$$

$$= \left[\frac{\text{Br} - \phi_0 N_{\text{outer}}(0)}{\text{Pe}} \right] \hat{z} + C \quad (32)$$

43 Here we employ higher-order matching since we're interested in the constant of integration for ϕ_1 . In this
44 case, the higher-order matching condition is $\lim_{z \rightarrow \infty} \delta^\beta \phi_1(z) = \frac{z}{z_{ct}} y_1$. So the matching condition from
45 Equation (25) is

$$\left[\frac{\text{Br} - \phi_0 N_{\text{outer}}(0)}{\text{Pe}} \right] z + C = -\frac{z}{z_{ct}} \frac{\text{Br} z_{ct}}{\kappa \alpha y_0^{\alpha-1} - \text{Pe}} \quad (33)$$

$$\implies \left[\frac{\text{Br} - \phi_0 N_{\text{outer}}(0)}{\text{Pe}} \right] + C = -\frac{\text{Br}}{\kappa \alpha y_0^{\alpha-1} - \text{Pe}} \quad (34)$$

46 Recall that $N_{\text{outer}}(0) = -\frac{\text{Br} \kappa \alpha \phi_0^{\alpha-2}}{\text{Pe} - \kappa \alpha \phi_0^{\alpha-1}}$. We plug this into Equation (34) such that

$$\left[\frac{\text{Br} - \phi_0 - \frac{\text{Br} \kappa \alpha \phi_0^{\alpha-2}}{\text{Pe} - \kappa \alpha \phi_0^{\alpha-1}}}{\text{Pe}} \right] + C = -\frac{\text{Br}}{\kappa \alpha y_0^{\alpha-1} - \text{Pe}} \quad (35)$$

$$\implies \frac{\text{Br}}{\text{Pe}} - \frac{\phi_0}{\text{Pe}} \left[-\frac{\text{Br} \kappa \alpha \phi_0^{\alpha-2}}{\text{Pe} - \kappa \alpha \phi_0^{\alpha-1}} \right] + C = -\frac{\text{Br}}{\kappa \alpha \phi_0^{\alpha-1} - \text{Pe}} \quad (36)$$

$$\implies \frac{\text{Br}}{\text{Pe}} - \frac{1}{\text{Pe}} \left[-\frac{\text{Br} \kappa \alpha \phi_0^{\alpha-1}}{\text{Pe} - \kappa \alpha \phi_0^{\alpha-1}} \right] + C = -\frac{\text{Br}}{\kappa \alpha \phi_0^{\alpha-1} - \text{Pe}} \quad (37)$$

$$\implies \frac{\text{Br}[\text{Pe} - \kappa \alpha \phi_0^{\alpha-1}] + \text{Br} \kappa \alpha \phi_0^{\alpha-1}}{\text{Pe}[\text{Pe} - \kappa \alpha \phi_0^{\alpha-1}]} + C = -\frac{\text{Br}}{\kappa \alpha \phi_0^{\alpha-1} - \text{Pe}} \quad (38)$$

$$\implies \frac{\text{Br}}{\text{Pe} - \kappa \alpha \phi_0^{\alpha-1}} + C = -\frac{\text{Br}}{\kappa \alpha \phi_0^{\alpha-1} - \text{Pe}} \quad (39)$$

$$\implies C = 0 \quad (40)$$

47 We then plug this C into Equation (24) to finalize our equation for the first-order solution of porosity:

$$\phi_1(\hat{z}) = \left[\frac{\text{Br} - \phi_0 N_{\text{outer}}(0)}{\text{Pe}} \right] \hat{z} + \frac{\phi_0}{\sqrt{a} \text{Pe}} [N_0 - N_{\text{outer}}(0)] \exp[-\sqrt{a} \hat{z}] \quad (41)$$

48 We can plug this into $\phi_{\text{inner}}(\hat{z}) = \phi_0(\hat{z}) + \delta^{\frac{1}{2}} \phi_1(\hat{z})$ to arrive at our inner solution for porosity:

$$\phi_{\text{inner}} = \phi_{\text{outer}}(0) + \delta^{\frac{1}{2}} \left[\left[\frac{\text{Br} - \phi_0 N_{\text{outer}}(0)}{\text{Pe}} \right] \hat{z} + \frac{\phi_0}{\sqrt{a} \text{Pe}} [N_0 - N_{\text{outer}}(0)] \exp[-\sqrt{a} \hat{z}] \right] \quad (42)$$

49 FINDING COMPOSITE SOLUTIONS

50 To find the composite solution for effective pressure, we consider the overlap region

$$\lim_{\hat{z} \rightarrow \infty} N_{\text{inner}}(\hat{z}) = \lim_{\tilde{z} \rightarrow 0} N_{\text{outer}}(\tilde{z}) = N_{\text{outer}}(0) \quad (43)$$

51 So the composite solution for effective pressure is

$$N_{\text{composite}} = N_{\text{outer}} + (N_0 - N_{\text{outer}}(0))\exp(-\sqrt{a}\hat{z}) \quad (44)$$

52 To find the composite solution for porosity, we consider the overlap region

$$\lim_{\hat{z} \rightarrow \infty} \phi_{\text{inner}}(\hat{z}) = \lim_{z \rightarrow 0} \phi_{\text{outer}}(z) \quad (45)$$

53 Recall from Equation (26) that we can expand the outer solution for small z . We take the expansion as
54 the matching condition such that

$$\lim_{\hat{z} \rightarrow \infty} \phi_{\text{inner}}(\hat{z}) = \lim_{z \rightarrow 0} \phi_{\text{outer}}(z) = \phi_{\text{outer}}(0) + \frac{z}{z_{ct}} \left[-\frac{\text{Br}z_{ct}}{\kappa\alpha\phi_0^{\alpha-1} - \text{Pe}} \right] \quad (46)$$

55 Therefore the composite solution of porosity combines Equations ?? and 42 and can be written as

$$\phi_{\text{composite}} = \phi_{\text{outer}} + \phi_{\text{inner}} - \left[\phi_{\text{outer}}(0) + \frac{z}{z_{ct}} \left[-\frac{\text{Br}z_{ct}}{\kappa\alpha\phi_0^{\alpha-1} - \text{Pe}} \right] \right] \quad (47)$$

56 SECTION B: COMPARISON TO NUMERICS FOR DIFFERENT SHEAR 57 HEATING RATE

58 Figure S1 shows comparison to numerics for $\text{Br} = 6$. The comparison shows good agreement with the ana-
59 lytical estimates presented in this study and the numerics for a different Brinkman number, and therefore
60 a different temperate zone thickness ($\sim 38\%$ of the ice thickness).

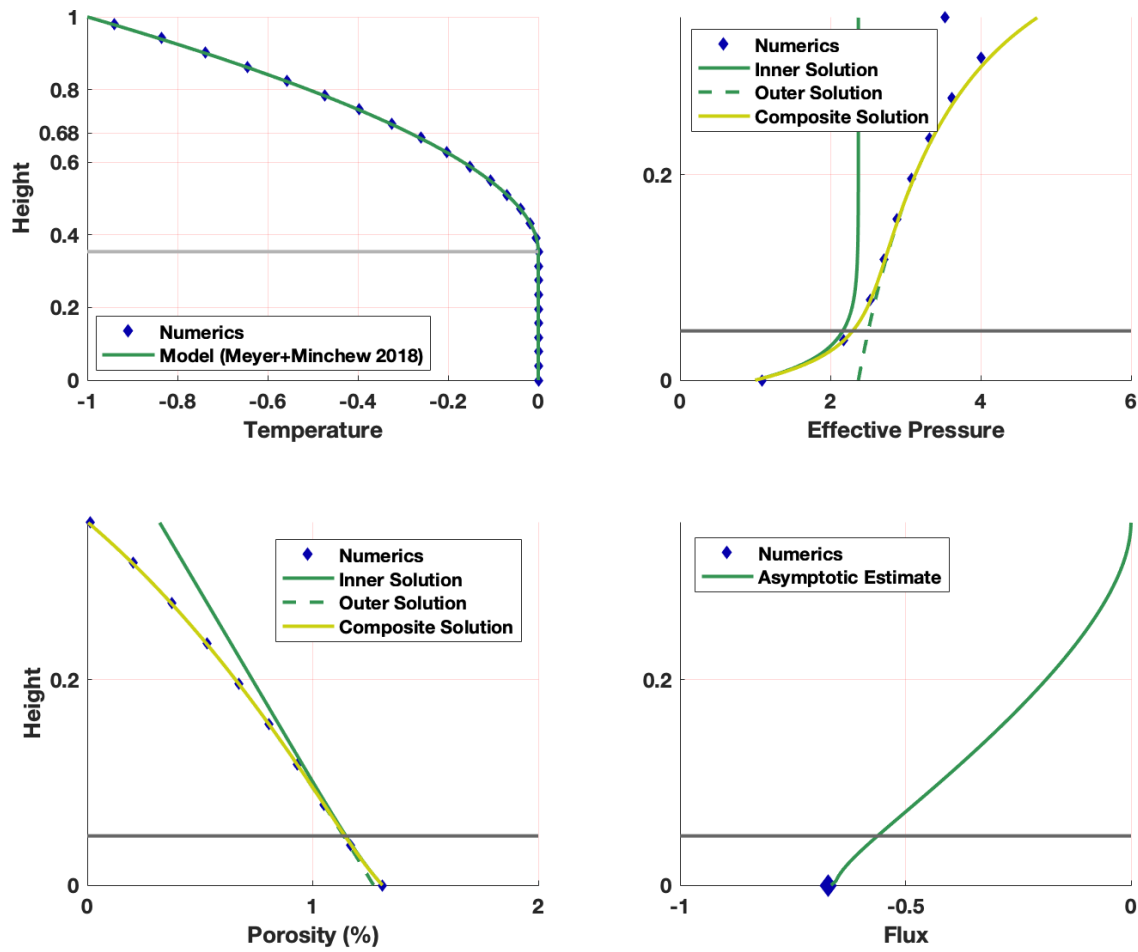


Fig. S1. Ice temperature, effective pressure, porosity, and meltwater flux, compared to numerics. In comparison to numerics, we let $H = 200$, $Pe = -1.1115$, $\kappa = 0.4416$, $Br = 6$, $\delta = 0.0023$, $\alpha = 2$, $\Delta T = 1$, $N_0 = 1$.

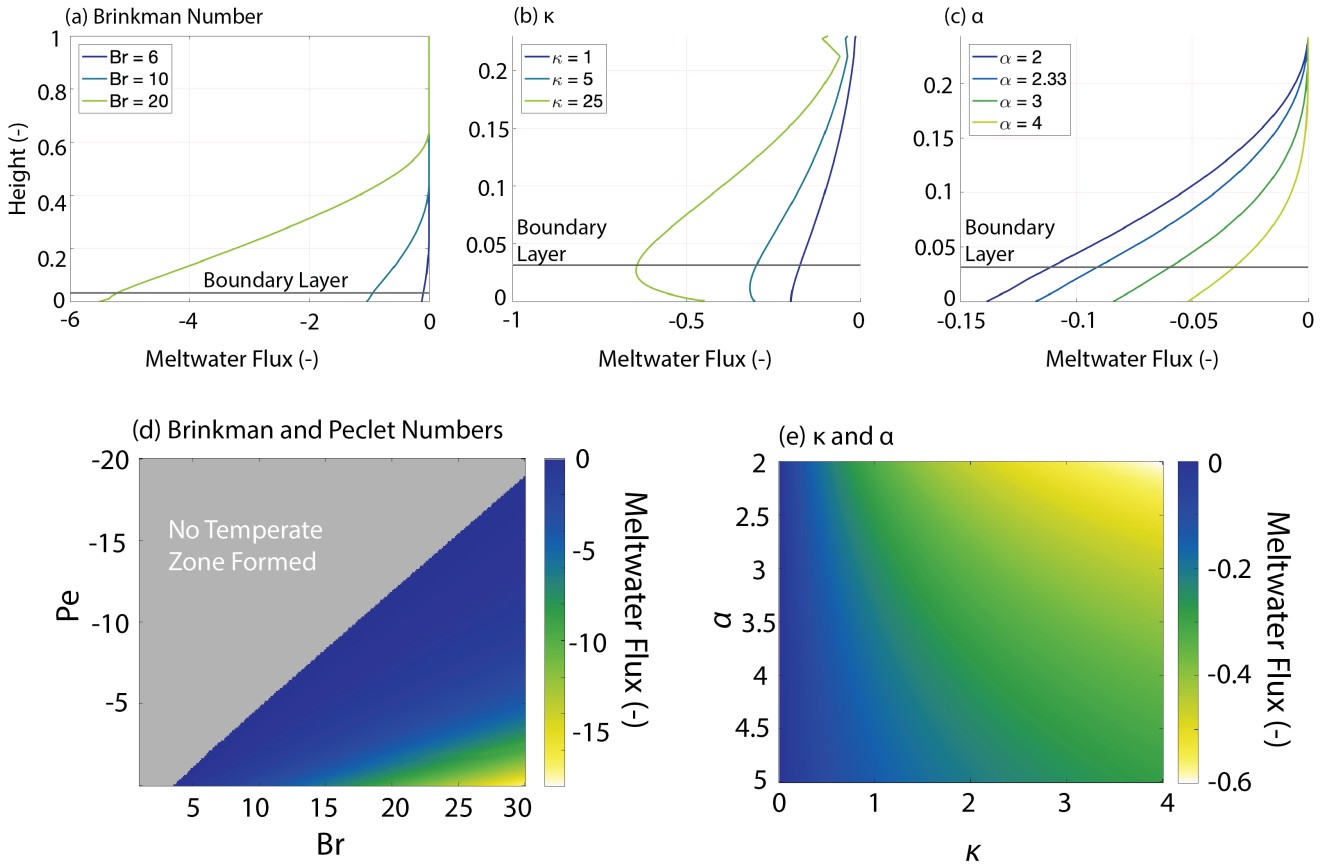


Fig. S2. Ice temperature, effective pressure, porosity, and meltwater flux, computed with varying parameters. The standard parameters are $h = 1000$ m, $Pe = -2.5$, $\kappa = 0.52$, $Br = 6$, $\delta = 0.001$, $\alpha = 2.5$, $\Delta T = 25$ K, $N_0 = 1$, and then specific parameters are varied: (a) Br, (b) κ , (c) α , (d) Br, Pe, (e) κ , α .

SECTION C: DEPENDENCE OF TEMPERATURE, PRESSURE, POROSITY, AND FLUX ON VARIOUS PARAMETERS

Here we show how ice temperature, effective pressure, ice porosity, and meltwater flux depends on the uncertain parameters explored in the main text. Figure S3a shows the profiles for varying Br, the Brinkman number. As discussed in the main text, the magnitude of flux is most sensitive to changes in this parameter. Further, this parameter affects the thickness of the temperature zone, effective pressure above the bed, and ice porosity at the bed.

Figure S3b shows the profiles for varying κ . Effective pressure varies significantly depending on the value of κ , though the change in porosity is much less. This leads to a smaller change in the flux.

Figure S3c shows results for varying δ . The parameter δ varies for many orders of magnitude and does not significantly affect porosity or meltwater flux. The difference in flux between orders of magnitude variations in δ is < 0.05 in nondimensional flux.

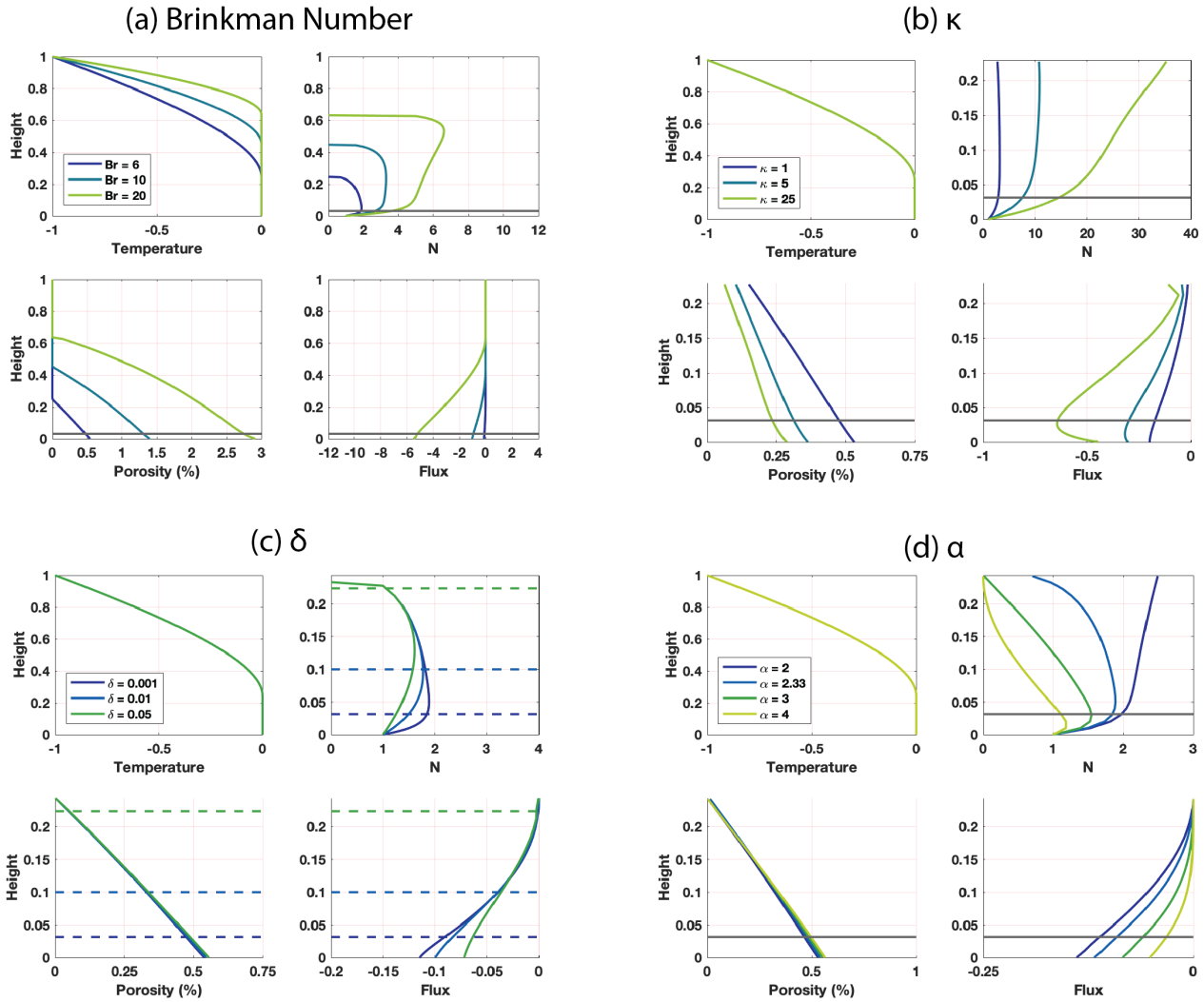


Fig. S3. Ice temperature, effective pressure, porosity, and meltwater flux, computed with varying parameters. The standard parameters are $h = 1000$ m, $Pe = -2.5$, $\kappa = 0.52$, $Br = 6$, $\delta = 0.001$, $\alpha = 2.5$, $\Delta T = 25$ K, $N_0 = 1$, and then specific parameters are varied: (a) Br , (b) κ , (c) δ , (d) α .

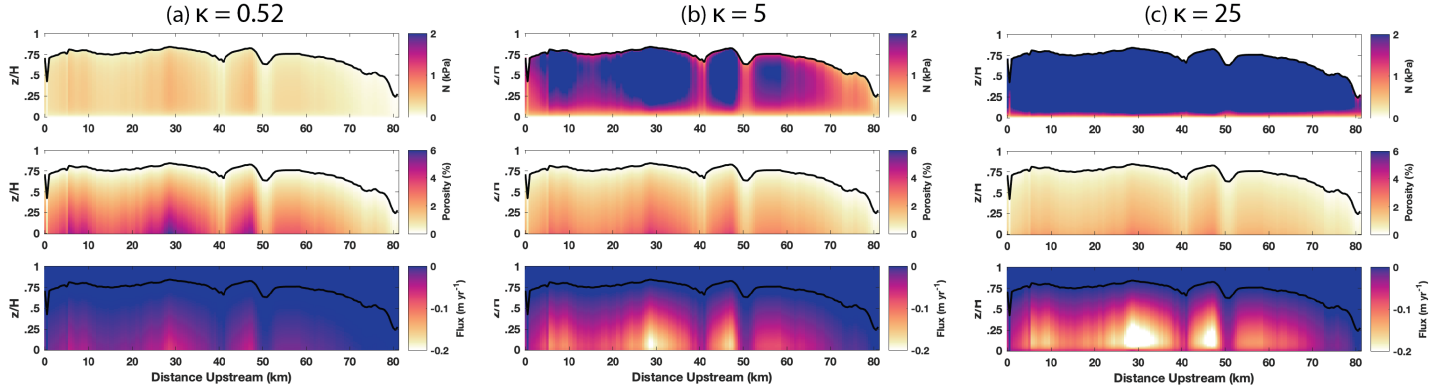
Depth profiles in Pine Island Glacier for a range of κ values

Fig. S4. Effect of varying κ on depth profiles in Antarctic ice streams: Estimates of effective pressure, porosity, and flux with depth for (a) $\kappa = 0.52$, (b) $\kappa = 5$, (c) $\kappa = 25$.

73 Finally, Figure S3d shows results for varying porosity exponent α . This parameter has a small effect
 74 on effective pressure and a negligible effect on ice porosity, leading to a very minor variation in meltwater
 75 flux for varying α .

76 SECTION C: EFFECT OF κ ON DEPTH PROFILES

77 As noted in the previous section, depth profiles (especially of effective pressure) vary with κ significantly,
 78 introducing uncertainty into the depth profiles of Antarctic ice streams shown in the main text. In Figure
 79 S4, we show depth profiles of Pine Island Glacier for three values of κ : $\kappa = 0.52$ (the value used in the
 80 main text), $\kappa = 5$, and $\kappa = 25$. These are values explored also in Schoof and Hewitt (2016).

81 SECTION D: EFFECT OF TEMPERATURE-VARYING A

82 In this study, we use a constant value for the ice softness parameter A , in which we define A to be the
 83 flow-rate parameter that corresponds to ice at its melting point. However, typically A is represented as a
 84 function of ice temperature T by

$$A = A_0 \exp \left[-\frac{Q}{RT} \right] \quad (48)$$

85 where Q is the activation energy for creep, R is the ideal gas constant, and A_0 is a constant prefactor. This
 86 parameter then enters the equation for ice flow as

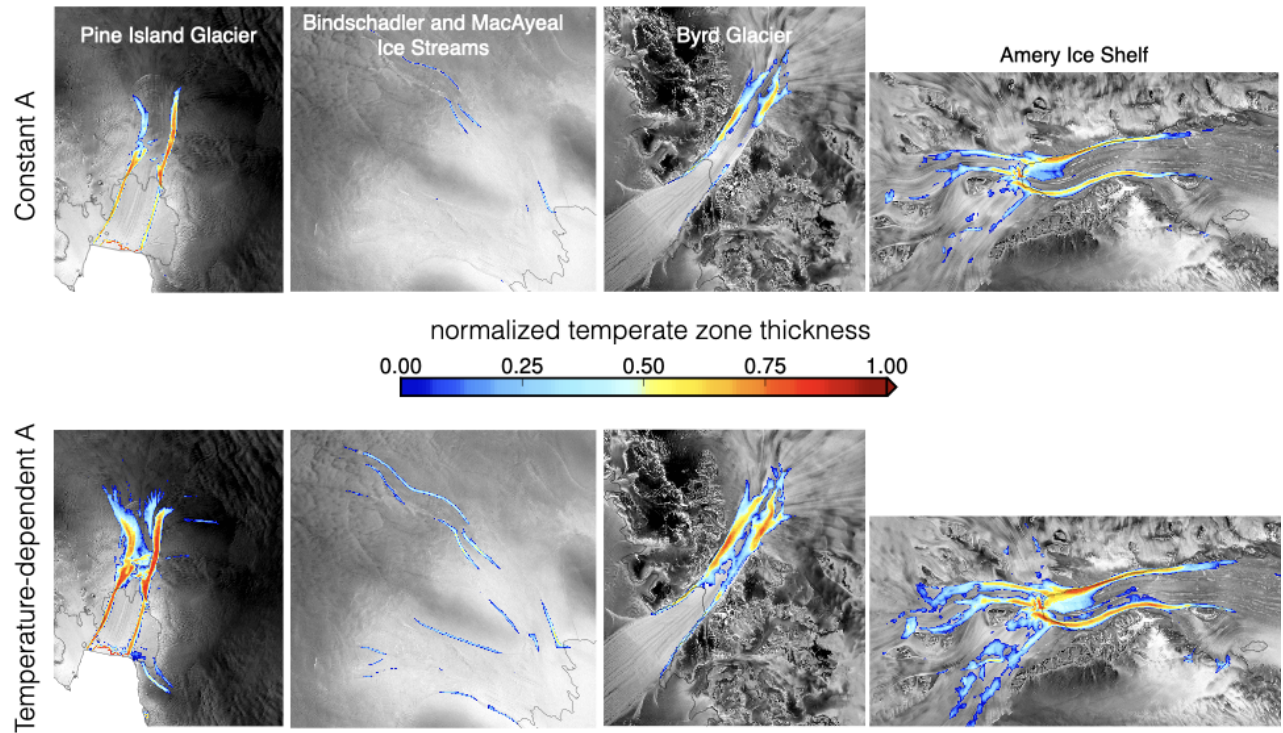


Fig. S5. Thickness of temperate ice zone, computed from the model presented in Meyer and Minchew (2018), for (top row) constant ice softness parameter A , and (bottom row) temperature-dependent ice softness parameter A .

$$\dot{\epsilon} = A\tau^n \quad (49)$$

87 where $\dot{\epsilon}$ is effective strain-rate, τ is effective deviatoric stress, and n is the stress exponent. In Figure S5, we
 88 show results for using a coupling between ice temperature and A . Including the temperature-dependent A
 89 results in larger and more extensive temperate ice zones in all regions studied, suggesting that this would
 90 produce larger meltwater fluxes than those presented in this study.

91 SECTION E: BRINKMAN AND PECKET NUMBERS IN ICE STREAMS

92 Estimates of ice temperature and thickness of temperate zone are dependent upon the nondimensional
 93 Brinkman number, denoted Br , and estimates of ice temperature, thickness of temperate zones, and melt-
 94 water flux are dependent upon the nondimensional Peclet number, denoted Pe . In Figure S6, we show
 95 these values, computed by the relations shown in the main text and from remote sensing observations.

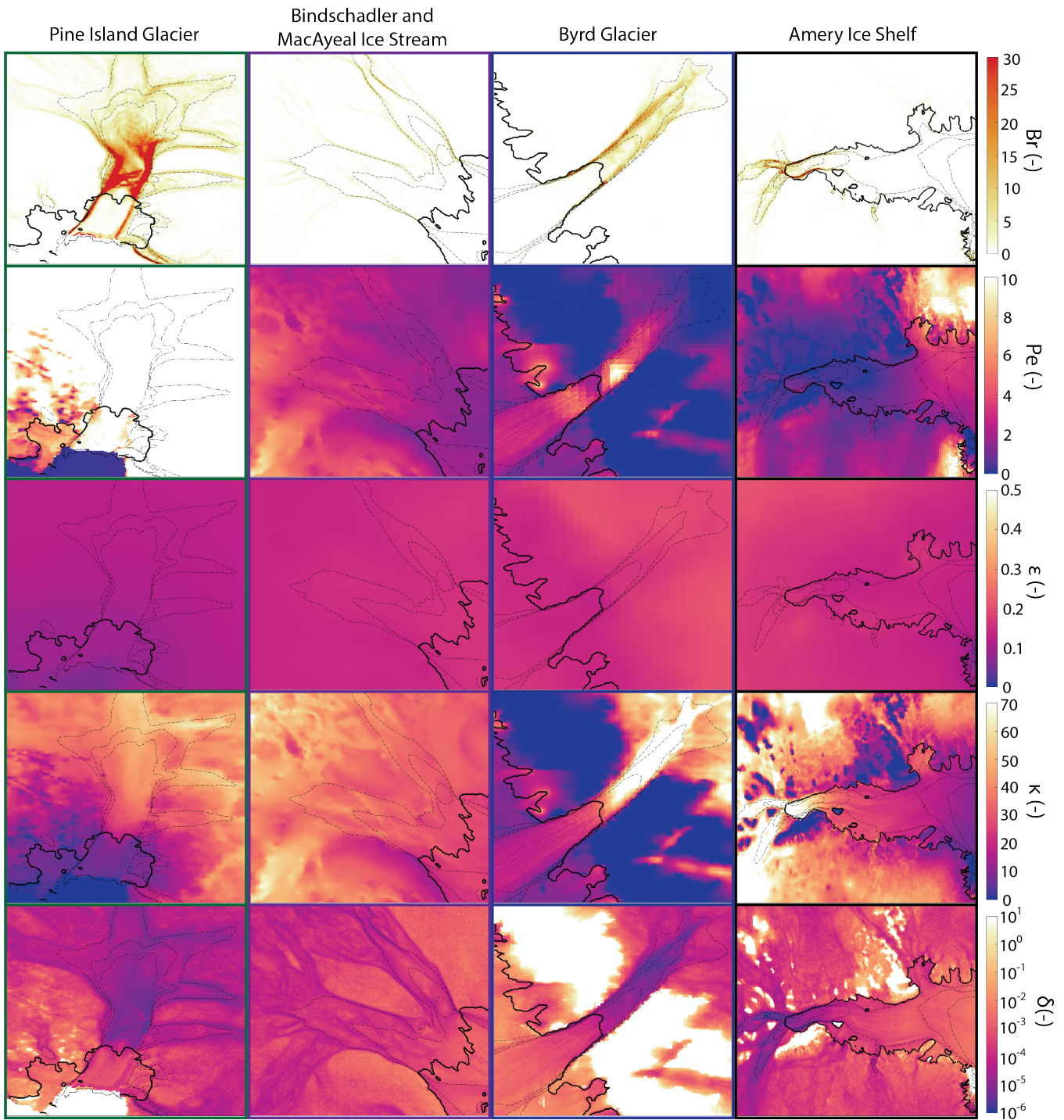


Fig. S6. Nondimensional in Antarctic ice streams: Brinkman number, Peclet number, ϵ , κ , δ computed for Pine Island Glacier, Bindschadler and MacAyeal Ice Streams, Byrd Glacier, and Amery Ice Shelf. Dashed lines denote velocity contours of 200 m yr⁻¹, 400 m yr⁻¹, 600 m yr⁻¹.

96 Br is larger in the shear margins due to the increase in strain-rate in these regions, thereby suggesting
97 that heating by viscous dissipation is strongest in these regions. Pe is dependent upon the vertical velocity,
98 here set to be $w = -a$, where a is surface accumulation. This varies based on the region of the ice streams,
99 with $\text{Pe} \sim 2 - 4$ except in Pine Island Glacier, where estimated surface accumulation rates are much higher
100 and therefore $\text{Pe} > 10$.

101 Further, estimates of porosity, effective pressure, and meltwater flux are dependent upon ϵ, κ, δ nondi-
102 mensional numbers defined in the main text. ϵ varies spatially based on surface temperature, while κ varies
103 based on ϵ and ice thickness, and δ varies based on ice thickness and a reference scale for ice viscosity.

104 **REFERENCES**

105 Meyer CR and Minchew BM (2018) Temperate ice in the shear margins of the Antarctic Ice Sheet: Controlling
106 processes and preliminary locations. *Earth and Planetary Science Letters*, **498**, 17–26 (doi: 10.1016/j.epsl.2018.
107 06.028)

108 Schoof C and Hewitt IJ (2016) A model for polythermal ice incorporating gravity-driven moisture transport. *Journal*
109 *of Fluid Mechanics*, **797**, 504–535, ISSN 0022-1120 (doi: 10.1017/jfm.2016.251)